PCCP

RSCPublishing

COMMUNICATION

Characterization and Preparation of Bio-Tubular Scaffolds for Fabricating Artificial Vascular by Combining Electrospinning and 3D Printing System

Cite this: DOI: 10.1039/x0xx00000x

Received 00th January 2012,
Accepted 00th January 2012

DOI: 10.1039/x0xx00000x

www.rsc.org/

Sang Jin Lee,[ab] Dong Nyoung Heo,[b] Ji Sun Park,[a] Seong Keun Kwon,[cde] Jin Ho Lee,[f] Jun Hee Lee,[a] Wan Doo Kim,[a] Il Keun Kwon‡*[b] and Su A Park‡*[a]

The last decade has seen artificial blood vessels composed of natural polymer nanofibers grafted into human bodies to facilitate the recovery of damaged blood vessels. However, electrospun nanofibers (ENs) of biocompatible materials such as chitosan (CTS) suffer from poor mechanical properties. This study describes the design and fabrication of artificial blood vessels composed of a blend of CTS and PCL ENs and coated with PCL strands using rapid prototyping technology. The resulting tubular vessels exhibited excellent mechanical properties and showed that this process may be useful for vascular reconstruction.

Surgical vascular repair is relatively common for replacing damaged or lost blood vessels due to trauma or vascular disease.[1] The number of artificial vascular bypass surgeries, including those used to repair coronary arteries or the damage caused by vascular disease, is 400,000 per annum.[2,3] Many biomedical engineering researchers are currently developing alternative strategies incorporating bio-functional materials for the regeneration of live blood vessels.[4] Elecrospun nanofibers (ENs), which can range in size from the sub-macroscale to the nanometer scale and are fabricated using an electrospinning (ELSP) method, are commonly used as biomaterial scaffolds due to their large surface area and ability to mimic the extracellular matrix.[5,6] Furthermore, ELSP can easily control the fibrous thickness and ENs have a high porosity.[7-9] These properties are important parameters for cells adhesion and proliferation within scaffolds.[4,6,10]

Among the various polymer nanofibers that have been developed, chitosan (CTS) ENs are particularly well-suited for regenerating various tissue because of the intrinsic bioaffinity of CTS, a natural amino polysaccharide (poly(1,4-D-glucosamine)). Commonly, CTS ENs are able to use biomedical scaffold for tissue reconstruction such as skin, bone, cartilage and vascular graft applications.[11] CTS EN is a kind of hydrophilic biomaterials which would swell in an aqueous environment. Therefore, it is very important to maintain the original fibrous structures for a long time when using these scaffolds. For this reason, neutralized-CTS ENs were used in order to maintain fibrous structure followed by that outcomes were used as tissue engineered bio-scaffold area and have been evaluated through *in vitro* or *in vivo* studies.[11-15] Recently, Fengyi Du et al.[16] and Min Zhou et al.[17] demonstrated the merits of artificial vascular systems composed of electrospun chitosan (CTS) blended with synthetic polycaprolactone (PCL) nanofibers in in vitro and in vivo studies. Both of the materials have been approved by the US Food and Drug Administration (FDA).[18] The introduction of PCL enhanced the physical strength of the artificial vessels. However, to obtain scaffolds with sufficient strength, the CTS content was reduced to levels that are unsuitable for healthy vascular repair. Additionally, artificial biocompatible vessels must be able to withstand high blood pressure, must not elicit an immune response, and should maintain the required form until full restoration with live vascular cells has been achieved.[19] Recently, the fabrication of solid free forms by rapid prototyping has received an enormous amount of attention. Rapid prototyping is a facile means of producing bio-compatible nanofiber scaffolds without the use of toxic solvents, and it allows the design of countless three-dimensional structures with controlled fiber size and spacing.[20-25] In this study, we designed and printed 3D artificial blood vessels composed of CTS/PCL ENs covered with PCL strands. This approach introduces a new paradigm with regard to the use of rapid prototyping for tubular vascular after 30 seconds.

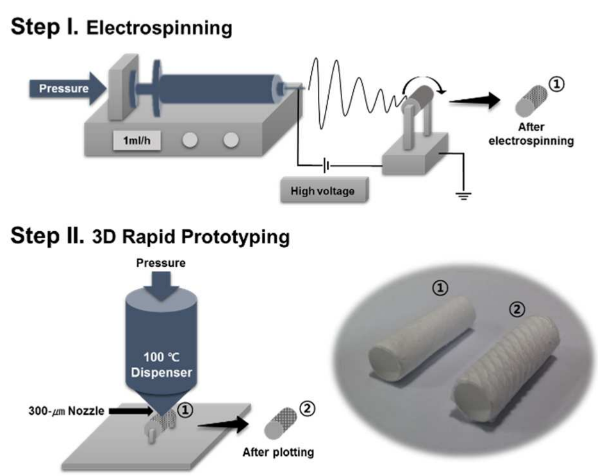

Fig. 1 Schematic illustration of the process used to fabricate 3D tubular artificial vascular scaffolds.

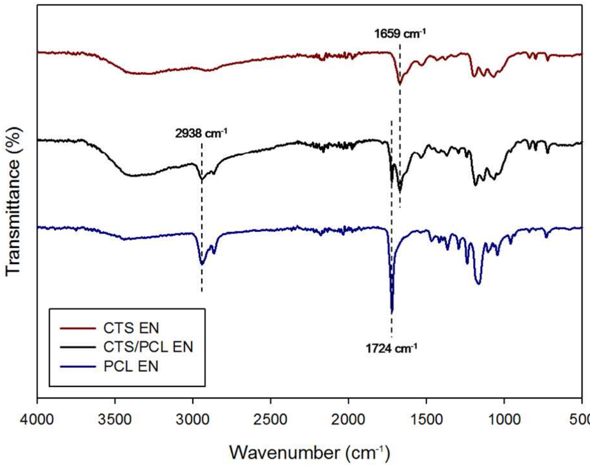

Fig. 2 Surface chemical properties of CTS (dark red), CTS/PCL (black), and PCL (dark blue) nanofiber scaffolds as characterized by FT-IR.

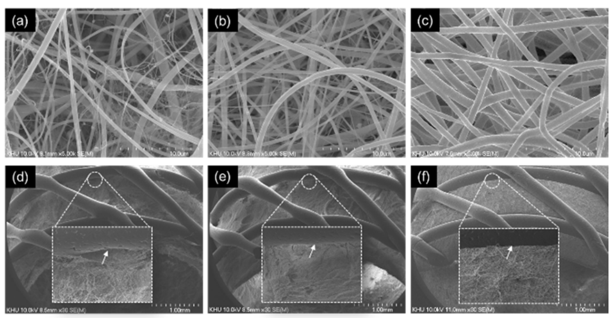

Fig 3. Scanning electron micrographs show the surface morphology of electrospun tubular (a) CTS nanofibers, (b) CTS/PCL nanofibers, (c) PCL nanofibers, (d) PCL-coated CTS nanofibers, (e) PCL-coated CTS/PCL nanofibers, and (f) PCL-coated PCL nanofibers.

scaffolds. As shown in Fig.1, CTS was blended with PCL tubular ENs, and the resulting composite was covered with tubular PCL strands, i.e., PCL coated.

The CTS blended with PCL was fabricated combining ELSP and rapid prototyping methods. The outcomes were characterized by Fourier transform infrared spectroscopy (FT-IR) and scanning electron microscopy (SEM). Surface contact angles, water absorption, and the mechanical properties of the artificial vessels were also evaluated. The detailed experimental procedure of including materials, methods, synthesis, and analytical equipment information were described in the electronic supplementary information (ESI).

The surface chemistry of the fabricated CTS and CTS/PCL ENs was analyzed by FT-IR absorbance. The spectrum of the CTS EN film shown in Fig.2 contains a characteristic peak at 1659 cm^{-1}, corresponding to an amide bond (N–H). The spectrum of PCL EN contained peaks corresponding to C–H bonds and an ester carbonyl group at 2938 cm^{-1} and 1725 cm^{-1}, respectively. The spectrum of CTS/PCL (9:1) EN contained bond amide and ester carbonyl peaks, indicating that CTS and PCL were well blended, as observed previously.[26] The SEM micrographs in Fig. 3a-c show the morphological characteristics of CTS, CTS/PCL, and PCL EN, respectively. CTS EN fibers were small in diameter and did not form a well-ordered topology. Conversely, micrographs of PCL EN showed a straight, well-ordered topology with larger fiber diameters. The micrograph of CTS/PCL EN shows a more ordered morphology than does CTS EN alone.[27] Blending the synthetic polymer into the natural polymer resulted in an even morphology indicative of a material that is well-suited to ELSP deposition.[26,28] The combined results of FT-IR and SEM analyses show that CTS and CTS/PCL EN tubes were successfully fabricated using an ELSP method.

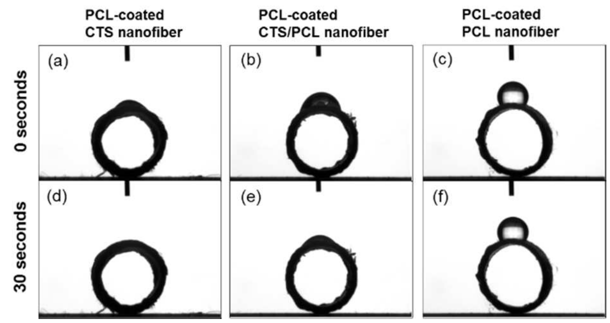

Fig. 4 Contact angles of water droplets are shown on (a, d) PCL-coated CTS nanofibers, (b, e) PCL-coated CTS/PCL nanofibers, and (c, f) PCL-coated PCL nanofibers.

The surface morphologies of the final products of the aforementioned procedure were characterized by SEM. The micrographs in Fig 3d-f show the three-dimensional, layer-by-layer structure of the PCL strands atop films of CTS, CTS/PCL, and PCL EN, respectively. The PCL strand diameter and inter-strand spacing were 300 um and 1200 um, respectively. The smaller micrographs in Fig. 3d-f show the boundary between the EN film and the overlaying strands. The micrograph in Fig. 3d shows that the CTS EN and PCL materials were not entirely compatible due to differences in their relative hydrophilicity.[29] Fig. 3e, however, shows that the CTS/PCL EN film was uniformly affixed to the PCL strands without a boundary gap. Furthermore, the PCL EN film and the overlaying PCL strands were also in full contact (Fig. 3f). Although PCL and CTS differ significantly in hydrophilicity and would not ordinarily mix evenly, the blended film acts as an interface layer that allows the two materials to come into intimate contact.[28,30] This type of contact is crucial to forming strong vascular scaffolds.

Fig. 4 shows contact angle measurements on each of the scaffold materials. The upper three photographs show a water droplet immediately after deposition. The lower three photographs were acquired after 30 seconds. Fig. 4a and d show that the PCL-coated CTS EN material had an initial contact angle of 44°, which was reduced to zero after 30 seconds. The PCL-coated CTS/PCL EN material had an initial contact angle of 79°, which decreased to 48°

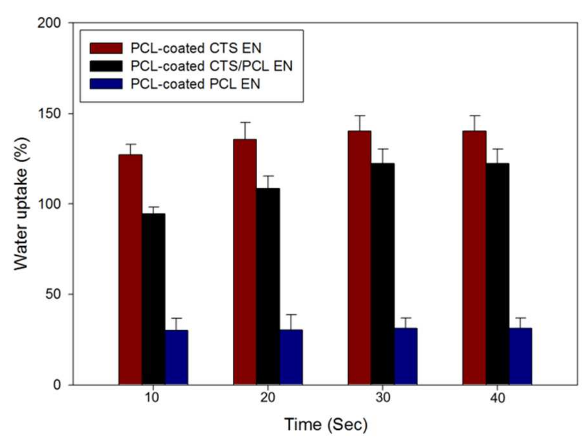

Fig. 5 Water absorption of PCL-coated CTS nanofibers (dark red), PCL-coated CTS/PCL nanofibers (black), and PCL-coated PCL nanofibers (dark blue).

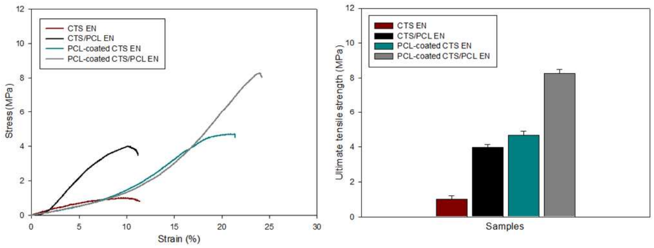

Fig. 6 Strain-stress curves (left) and ultimate tensile strengths (right) of tubular nanofibers and PCL-coated tubular nanofibers.

In both cases, the decrease in contact angle is indicative of water absorption. In contrast, the PCL-coated PCL EN material had an initial contact angle of 113°, which remained unchanged. These results confirm the relatively high hydrophobicity of PCL. Thus, one may expect differences in the water absorption properties of these materials as a function of PCL content.[29]

Fig. 5 and Fig. S2 (ESI, †) show that the PCL-coated CTS EN material absorbed approximately 13% more water between 10 and 40 seconds of exposure. Similarly, the PCL-coated CTS/PCL EN material showed a 28% increase in water absorption between 10 and 40 seconds of exposure. In contrast, the stable contact angle of the PCL-coated PCL EN material indicates that no water was absorbed, likely due to the hydrophobic nature of the material. Furthermore, after 30 sec, the PCL-coated CTS EN scaffold absorbed approximately 18% more water than did the PCL-coated CTS/PCL EN materiall. Additionally, the absorption rate did not noticeably increase beyond 30 seconds both PCL-coated CTS EN and PCL-coated CTS/PCL EN. This phenomenon meaning is that materials of final equilibrium of water uptake are 30 sec. This is likely due to the higher CTS content in the CTS EN. Previous reports have demonstrated that the wettability and relative hydrophilicity of a polymer surface are determining factors of the degree of cell adhesion and migration.[31-33] Thus, the high CTS content of the tubular, PCL-coated CTS EN scaffolds described herein allows for good cell adhesion and proliferation.[34]

Fig. 6 and Fig. S3 (ESI, †) show the results of curves of strain-stress and ultimate tensile testing of each material. As shown in the tensile stress–strain curves, there is considerably difference depending on an increasing of PCL content or PCL coating onto fabricated ENs.[35] Additionally, the ultimate tensile strength of pure CTS EN was considerably lower than that of PCL-coated CTS EN, and that of CTS/PCL EN was much lower than that of PCL-coated CTS EN. These results indicate that the strength of the scaffold increases significantly with the presence of the PCL strand coating. Previous reports state that the ultimate tensile strengths of intact carotid artery and human left internal mammary arteries are 2.59 ± 0.31 MPa and 4.3 ± 1.8, respectively.[36,37] The ultimate tensile strength of coronary arteries can range from 1.40 to 11.14 MPa.[4] When vascular regeneration is needed, the use of components made only of EN is difficult due to the variable strength requirements of native blood vessels. The above results show that the method described herein may be useful as a means of producing strong artificial vessels.

Conclusions

In summary, novel and strong artificial blood vessels were fabricated using ELSP and a 3D bioprinting system. CTS, PCL, and blended CTS/PCL EN scaffolds were fabricated and evaluated by FTIR and SEM. Water absorption, and therefore hydrophilicity, increased with increasing proportions of CTS. The fabricated tubular scaffolds were suitable in terms of both surface morphology and mechanical properties, both of which were significantly enhanced by the printing of PCL strands on the EN substrate. Our results demonstrate the synthesis of artificial vessels composed of EN reinforced with 3D-printed PCL strands.

Acknowledgement

This study was supported by a grant from the Korean Health Technology R&D Project, (HI14C01840300) Ministry of Health & Welfare, Republic of Korea.

Notes

[a]*Department of Nature-Inspired Nanoconvergence Systems, Korea Institute of Machinery and Materials, 156 Gajeongbuk-ro, Yuseong-gu, Daejeon 304-343, Republic of Korea*
[b]*Department of Maxillofacial Biomedical Engineering and Institute of Oral Biology, School of Dentistry, Kyung Hee University, 26 Kyunghee-daero, Dongdaemun-gu, Seoul 130-701, Republic of Korea*
[c]*Department of Otorhinolaryngology, Head and Neck Surgery, 101 Daehak-ro, Jongno-gu, Seoul National University Hospital, Seoul 110-744, Republic of Korea*
[d]*Cancer Research Institute, Seoul, Republic of Korea*
[e]*Seoul National University Medical Research Center, Seoul, Republic of Korea*
[f]*Department of Advanced Materials, Hannam University, 461-6 Jeonmin Dong, Yuseong-gu, Daejeon 305-811, Republic of Korea*
† Electronic Supplementary Information (ESI) available: The detailed experimental procedures, equipment, and measured value. See DOI: 10.1039/c000000x/
‡ These corresponding authors made equal contributions to this work.

References

1. S. J. Lee, J. J. Yoo, G. J. Lim, A. Atala and J. Stitzel, *J. Biomed. Mater. Res. Part A*, 2007, **83**, 999-1008.
2. S. Kaushal, G. E. Amiel, K. J. Guleserian, O. M. Shapira, T. Perry, F. W. Sutherland, E. Rabkin, A. M. Moran, F. J. Schoen and A. Atala, *Nature medicine*, 2001, **7**, 1035-1040.
3. T. Huynh, G. Abraham, J. Murray, K. Brockbank, P.-O. Hagen and S. Sullivan, *Nature biotechnol.*, 1999, **17**, 1083-1086.
4. C. Xu, R. Inai, M. Kotaki and S. Ramakrishna, *Tissue. Eng.*, 2004, **10**, 1160-1168.
5. X. Zhang, V. Thomas, Y. Xu, S. L. Bellis and Y. K. Vohra, *Biomaterials*, 2010, **31**, 4376-4381.
6. S. Agarwal, J. H. Wendorff and A. Greiner, *Adv. Mater.*, 2009, **21**, 3343-3351.
7. J. Venugopal, S. Low, A. T. Choon and S. Ramakrishna, *J. Biomed. Mater. Res. Part A*, 2008, **84**, 34-48.
8. Y. A. Dzenis, Science, 2004, **304**, 1917-1919
9. K. A. Rieger, N. P. Birch and J. D. Schiffman, *J. Mater. Chem. B*, 2013, **1**, 4531-4541.
10. S. R. Bhattarai, N. Bhattarai, H. K. Yi, P. H. Hwang, D. I. Cha and H. Y. Kim, *Biomaterials*, 2004, **25**, 2595-2602.

11. F. Ding, H. Deng, Y. Du, X. Shi and Q. Wang, *Nanoscale*, 2014, **6**, 9477-9493.
12. P. Sangsanoh and P. Supaphol, *Biomacromolecules*, 2006, **7**, 2710-2714.
13. P. Sangsanoh, O. Suwantong, A. Neamnark, P. Cheepsunthorn, P. Pavasant and P. Supaphol, *Euro. Polym. Jour.*, 2010, **46**, 428-440.
14. V. T. Tchemtchoua, G. Atanasova, A. Aqil, P. Filée, N. Garbacki, O. Vanhooteghem, C. Deroanne, A. Noël, C. Jérome and B. Nusgens, *Biomacromolecules*, 2011, **12**, 3194-3204.
15. S. C. Neves, L. S. Moreira Teixeira, L. Moroni, R. L. Reis, C. A. Van Blitterswijk, N. M. Alves, M. Karperien and J. F. Mano, *Biomaterials*, 2011, **32**, 1068-1079.
16. F. Du, H. Wang, W. Zhao, D. Li, D. Kong, J. Yang and Y. Zhang, *Biomaterials*, 2012, **33**, 762-770.
17. M. Zhou, W. Qiao, Z. Liu, T. Shang, T. Qiao, C. Mao and C. Liu, *Tissue Eng. Part A*, 2013, **20**, 79-91.
18. H.-J. Shao, Y.-T. Lee, C.-S. Chen, J.-H. Wang and T.-H. Young, *Biomaterials*, 2010, **31**, 4695-4705.
19. C. H. Mun, Y. Jung, S.-H. Kim, S.-H. Lee, H. C. Kim, I. K. Kwon and S. H. Kim, *Tissue Eng. Part A*, 2012, **18**, 1608-1616.
20. K. C. Hung, C. S. Tseng and S. h. Hsu, *Adv. Health. Mater.*, 2014, **3**, 1578-1587.
21. F. P. Melchels, M. A. Domingos, T. J. Klein, J. Malda, P. J. Bartolo and D. W. Hutmacher, *Prog. Polym. Sci.*, 2012, **37**, 1079-1104.
22. T. Y. Tu, Z. Wang, J. Bai, W. Sun, W. K. Peng, R. Y. J. Huang, J. P. Thiery and R. D. Kamm, *Adv. Health. Mater.*, 2014, **3**, 609-616.
23. T. G. Kim, H. Shin and D. W. Lim, *Adv. Func. Mater.*, 2012, **22**, 2446-2468.
24. Y. Luo, A. Lode and M. Gelinsky, *Adv. Health. Mater.*, 2013, **2**, 777-783.
25. S. V. Murphy and A. Atala, *Nature biotech.,* 2014, **8**, 773-785
26. K. Shalumon, K. Anulekha, C. Girish, R. Prasanth, S. Nair and R. Jayakumar, *Carbohyd. Polym.*, 2010, **80**, 413-419.
27.Y. Yao, J. Wang, Y. Cui, R. Xu, Z. Wang, J. Zhang, K. Wang, Y. Li, Q. Zhao and D. Kong, Acta Biomater., 2014, 10, 2739-2749.
28. A. Sionkowska, *Prog. Polym. Sci.*, 2011, **36**, 1254-1276.
29. Y. Ji, K. Liang, X. Shen and G. L. Bowlin, *Carbohyd. Polym.*, 2014, **101**, 68-74.
30. V. N. Malheiro, S. G. Caridade, N. M. Alves and J. F. Mano, *Acta Biomater.*, 2010, **6**, 418-428.
31. M. Lampin, R. Warocquier-Clérout, C. Legris, M. Degrange and M. Sigot-Luizard, *J. Biomed. Mater. Res.*, 1997, **36**, 99-108.
32. Y. Arima and H. Iwata, *Biomaterials*, 2007, **28**, 3074-3082.
33. D. L. Elbert and J. A. Hubbell, *Annu. Rev. Mater. Sci.*, 1996, **26**, 365-394.
34. J. Zhao, H. Qiu, D.-l. Chen, W.-x. Zhang, D.-c. Zhang and M. Li, *Int. J. Biol. Macromol.*, 2013, **56**, 106-113.
35. W. Yang, J. Fu, D. Wang, T. Wang, H. Wang, S. Jin and N. He, *J. Biomed. Nanotechnol.*, 2010, **6**, 254-259.
36. K. A. McKenna, M. T. Hinds, R. C. Sarao, P.-C. Wu, C. L. Maslen, R. W. Glanville, D. Babcock and K. W. Gregory, *Acta Biomater.*, 2012, **8**, 225-233.
37. M. Stekelenburg, M. C. Rutten, L. H. Snoeckx and F. P. Baaijens, *Tissue Eng. Part A*, 2008, **15**, 1081-1089.